Two Different Regimes of Anomalous Walker Circulation over the Indian and Pacific Oceans before and after the Late 1970s

Ryuichi Kawamura[1], Hiromitsu Aruga[1], Tomonori Matsuura[2] and Satoshi Iizuka[2]

[1]Department of Earth Sciences, Toyama University, Toyama, Japan

[2]National Research Institute for Earth Science and Disaster Prevention, Tsukuba, Ibaraki, Japan

Submitted to the AGU book entitled "Ocean-Atmosphere interaction and Climate Variability"

August 25, 2003

Corresponding author address: Dr. Ryuichi Kawamura, Department of Earth Sciences, Toyama University, 3190 Gofuku, Toyama 930-8555, Japan.

E-mail: kawamura@sci.toyama-u.ac.jp

Abstract

Using the National Centers for Environmental Prediction/National Center for Atmospheric Research reanalysis data aided by a coupled ocean-atmosphere model, we investigated two different regimes of anomalous Walker circulation system over the Pacific and Indian Oceans before and after a climate shift, occurred in the late 1970s, in terms of cross-basin connection.

During the period before the climate shift when tropospheric biennial oscillation (TBO)-like El Nino-Southern Oscillation (ENSO) dominates, which is termed the TBO-like ENSO regime, it is apparent that anomalous rainfall and upper-level velocitiy potential systematically move eastward from the tropical Indian Ocean to the warm pool region of the western Pacific during the growth phase of ENSO. In the meantime, the activities of South Asian and Australian summer monsoon systems are directly affected by the evolution of the anomalous Walker circulation. The model captures similar systematic eastward propagation and model results show that westerly wind bursts over the warm pool region of the western Pacific contribute significantly to the onset of model warm event through the excitation of downwelling equatorial Kelvin waves. It is found that the cross-basin connection between the tropical Indian and Pacific Oceans is prerequisites for the turnabout of the TBO-like ENSO because the frequent occurrence of the westerly wind bursts depends strongly on the phase transition of the anomalous Walker circulation over the two ocean basins.

During the period after the climate shift when prolonged ENSO occurs frequently, which is termed the prolonged ENSO regime, it is observed that a upper-level velocitiy potential anomaly in the vicinity of the Philippine Sea and maritime continent expand westward into the northern Indian Ocean and South Asia during the decay phase of ENSO, accompanied by a noticeable rainfall anomaly over the Indian Ocean, which is identified with a major precursory signal of anomalous South Asian summer monsoon in the preceding spring. However, the model fails to reproduce such westward expansion. Since a positive

wind-evaporation-SST (WES) feedback, prevailing in spring over the tropical Indian Ocean, is at least a partial cause of this westward progression, the model failure may result from the absence of a pronounced off-equatorial SST anomaly in spring over the Philippine Sea that possibly triggers a WES mode through the westward propagation of atmospheric Rossby waves in response to equatorially asymmetric convective heating anomalies around the maritime continent.

It is concluded that the cross-basin connection between the two ocean basins is apparently different between the two regimes of the anomalous Walker circulation system before and after the late 1970s. It is also suggested that this difference may have led to the controversial results on the lag relationship between the South Asian summer monsoon and ENSO and might also be one of the possible reasons why the changes in ENSO properties occurred around the late 1970s.

1. Introduction

It has been recognized that the significant changes in the El Nino-Southern Oscillation (ENSO) properties occurred around the late 1970s in terms of its periodicity and seasonality [e.g., *Wang,* 1995; *Mitchell and Wallace,* 1996; *Wang and An,* 2002]. Associated with this phenomenon, it has also been reported that the South Asian summer monsoon-ENSO relationship through the Walker circulation evidently changed before and after the late 1970s [e.g., *Kumar et al.,* 1999; *Torrence and Webster*, 1999; *Miyakoda et al.,* 2000; *Krishnamurthy and Goswami,* 2000; *Kinter et al.,* 2002]. The variability of the western North Pacific summer monsoon [*Murakami and Matsumoto,* 1994] and the associated anomalous East Asian summer climate are also significantly different before and after that period [*Kawamura et al.,* 1998; *Wang et al.,* 2001; *Wu and Wang,* 2002].

A number of researchers have already pointed out a significant coupling of the South Asian monsoon and ENSO [e.g., *Angell,* 1981; *Shukla and Paolino,* 1983; *Rasmusson and Carpenter,* 1983; *Meehl,* 1987; *Webster and Yang,* 1992; *Ju and Slingo,* 1995; *Webster et al.,* 1998]. *Barnett* [1983; 1984] and *Yasunari* [1985; 1990; 1991] postulated that zonal propagation of anomalous Walker circulation from the Indian Ocean to the Pacific Ocean region is intimately associated with ENSO, based on observational data before the early 1980s. They emphasized the active role of the Asian monsoon variability in triggering ENSO events because a weak (strong) Asian summer monsoon preceded a warm (cold) event of ENSO prevailing in boreal winter.

After the late 1970s, on the contrary, a warm (cold) event of ENSO tended to precede a weak (strong) Asian summer monsoon so far as broad-scale monsoon circulation indices, such as *Webster and Yang* [1992] index, are used as a measure of the monsoon intensity. *Yang et al.* [1996] and *Yang and Lau* [1998] pointed out that the ENSO in the preceding winter and spring have an indirect impact on the summer monsoon activity through land surface hydrologic processes in the Asian continent, as well as a direct impact of ENSO. *Kawamura* [1998] showed that enhanced convective heating over the northern Indian Ocean with an ENSO signal induces anomalous upper-level anticyclonic circulation as a result of the Rossby wave response, thereby decreasing rainfall and increasing near-surface temperature in central and southwest Asia in spring prior to a strong South Asian summer monsoon. Based on observational data after the late 1970s, they emphasized the active role of ENSO in affecting the Asian summer monsoon variability.

Li and Zhang [2002] noted that these controversial results might arise from the different-period datasets they used for their analyses. It is still uncertain, however, why the changes in the monsoon-ENSO relationship concurred with those in ENSO properties. Some researchers postulated that the recent weakening of the Indian summer rainfall-ENSO connection might be attributed to the strengthening and poleward shift of the jet stream over the

North Atlantic [*Chang et al.,* 2001], or the frequent occurrence of intense Indian Ocean dipole mode [*Ashok et al.,* 2001]. Their possible mechanisms on the monsoon-ENSO relationship do not necessarily require the changes in ENSO properties. On the other hand, *Wang and An* [2002] suggested a possible role of the Pacific climate shift in the decadal changes of ENSO properties. *Kinter et al.* [2002] stressed that the decadal change in North Pacific sea surface temperature (SST) and the associated change in the overlying atmospheric circulation are linked with the weakening in the monsoon-ENSO relationship. If their ideas are correct, the Pacific climate shift is responsible for the changes in both ENSO properties and monsoon-ENSO relationship.

Another possibility is that the significant changes in ENSO properties in the late 1970s might have caused those in the monsoon-ENSO relationship. Delayed and indirect impacts of ENSO at its decay phase on the summer monsoon system have been highlighted by *Yang and Lau* [1998], *Shen et al.* [1998], *Wang et al.* [2000; 2001], and *Kawamura et al.* [2001a, b], whereas direct impacts of ENSO at its growth phase have been demonstrated by *Chen and Yen* [1994], *Ju and Slingo* [1995], *Lau and Wu* [2001], and *Kawamura et al.* [2003]. These studies suggest that the indirect ENSO impacts on the monsoon system at the decay phase of ENSO are quite different from those at its growth phase. Since the seasonality of ENSO cycle changes before and after the late 1970s [*Mitchell and Wallace,* 1996], the differences in ENSO impacts between its growth and decay phases are very likely to affect the monsoon-ENSO relationship.

According to *Kawamura et al.* [2003] who examined a direct ENSO impact at its growth phase on the South Asian summer monsoon interannual variability during the period prior to the late 1970s, a combination of the tropical ocean-atmosphere interactions over both the Indian and Pacific sectors is crucial for the turnabout of anomalous Walker circulation system relevant to the regular phase change of ENSO. It seems that such a turnabout over the two ocean basins considerably changed after the late 1970s. However, few studies focus specifically on its regime transition before and after the late 1970s in terms of the cross-basin

connection between the tropical Indian and Pacific Oceans, although the Walker circulation over the Pacific Ocean basin has well been examined in association with ENSO theories [e.q., *Schopf and Suarez,* 1988; *Weisberg and Wang,* 1997; *Jin,* 1997]. A proper understanding of its cross-basin connection might be important in clarifying why the changes in ENSO properties occurred around the late 1970s and why the controversial results were obtained on the lag relationship between the South Asian monsoon and ENSO.

In section 2, we introduce the model simulation and the datasets used in this study. Section 3 demonstrates the remarkable observed features of the anomalous Walker circulation system over the tropical Indian and Pacific Oceans before and after the late 1970s. In sections 4 and 5, we examine ENSO-like phenomena simulated in a coupled ocean-atmosphere model (CGCM) and discuss the similarities and discrepancies between model results and observations in terms of the cross-basin connection between the two ocean basins. A summary is provided in section 6.

2. Data used and analysis procedure

To examine the observed behavior of anomalous Walker circulation over the two ocean basins, we use the National Centers for Environmental Prediction/National Center for Atmospheric Research (NCEP/NCAR) global atmospheric reanalysis dataset [*Kalnay et al.,* 1996]. First, we apply an empirical orthogonal function (EOF) analysis to the tropical SSTs derived from the Global Ice and SST (GISST) dataset [*Parker et al.,* 1995] and extract dominant SST anomaly patterns during two 15-yr periods before and after the late 1970s. As is well known, the first 15-yr period 1962-1976 is the period when tropospheric biennial oscillation (TBO)-like ENSO dominates, whereas another 15-yr period 1979-1993 is characterized by the dominance of prolonged ENSO with a 4-5 yr periodicity [e.g., *Torrence and Webster,* 1999; *Li and Zhang,* 2002; *Kawamura et al.,* 2003]. For convenience, the former and latter periods are hereafter called period I and II, respectively. Second, a

lag-regression analysis is conducted to investigate the coupling between the leading SST mode and the anomalous Walker circulation.

In this study we also analyze the model output of a CGCM developed at the National Research Institute for Earth Science and Disaster Prevention [*Iizuka et al.,* 2003]. The atmospheric component of the CGCM used in this study is the Japan Meteorological Agency global spectral model (JMA-GSM8911). The atmospheric model uses triangular truncation at wave number 42. There are 21 levels in the vertical from the surface to about 10 hPa. The model includes comprehensive physical parameterizations. A detailed description of the physical processes is provided in *Sugi et al.* [1990]. The convection scheme is the mass flux scheme proposed by *Arakawa and Schubert* [1974], which is modified for entrainment rate and for determination of mass flux at cloud base. The details of the prognostic Arakawa-Schubert scheme (PAS) are provided in *Kuma* [1996]. The ocean component of the CGCM is based on the Geophysical Fluid Dynamics Laboratory Modular Ocean Model 2.2 [*Pacanowski*, 1996]. The horizontal grid spacing is 1.125º longitude by 0.5625º latitude. There are 37 levels in vertical; the upper 400 m is divided into 25 levels. *Pacanowski and Philander's* [1981] parameterization is used in determining the coefficient of vertical mixing. The ocean model is spun up for 10 years from a static state using *Levitus* [1982] annual mean temperatures and salinities as initial conditions, and then coupled with the atmospheric model without flux corrections. The CGCM is run for 20 years, but only output for the last 15 years is analyzed when the trend in the equatorial SST is relatively small.

3. Observed ENSO regimes

3.1 Dominant SST patterns

Figure 1 shows the spatial patterns and time series of the first SST modes appearing in the Pacific sector during northern winter (December-January) for period I and II, which are derived from the application of a simple EOF analysis to monthly SST anomaly data. Note

that the winter 1993 refers to the period from December 1992 through February 1993. Also exhibited are those of model SST. The first mode for period I accounts for 43% of the total variance and has a 2-3 yr periodicity, whereas for period II the percentage variance goes down to 25% and its periodicity shifts toward longer timescales. Their spatial patterns are very similar to each other, capturing dominant features of ENSO, but there is a significant difference in the Philippine Sea SST anomaly between the two periods in terms of its magnitude. A positive SST anomaly east of the Philippines is more evident after the late 1970s than before that. It turns out, on the other hand, that the CGCM is successful in simulating the basic features of ENSO-related SST anomalies. The periodicity of the first mode in the model SST field is around 3-4 years, which is comparable to observations, and its spatial pattern is also similar to that observed.

In the following subsections, we show the spatial distributions of lag-regression coefficients of SST and atmospheric variables with the time series of each first SST mode in northern winter. Note that the lag-regression analysis is performed on a seasonal mean basis.

3.2 TBO-like ENSO regime

Figure 2 shows the lag-regression maps of SST with the time series of the wintertime first mode during period I for September-November (lag-1), December-February (lag0), March-May (lag+1), and June-August (lag+2). The “lag-1”, “lag0” and “lag+1” denote the preceding season, the reference season and the subsequent season, respectively. In this figure, fall season (SON) corresponds to the growth phase of the cold event of ENSO. When the cold event develops, a negative SST anomaly is indicated over the tropical Indian Ocean and persist until the subsequent spring (MAM), while in SON a weak positive SST anomaly over the Philippine Sea becomes dissipated rapidly. A positive SST anomaly over the Arafura Sea and Timor Sea in the same season is also replaced with a negative one in winter (DJF). After the mature phase of the cold event, a positive SST anomaly appears off the coast of Peru in MAM,

implying the onset phase of a warm event, and further develops in summer (JJA). Thus, MAM is the transition phase of ENSO during period I [e.g., *Rasmusson and Carpenter,* 1982]. Since the ENSO cycle is considerably regular and has a 2-3 yr period, as seen in Fig. 1, we term ENSO-related circulation features, prevailing prior to the late 1970s, TBO-like ENSO regime. Note that in the present study, we consider the TBO component as one of ENSO properties [e.g., *Meehl,* 1987; 1993].

In the same way, the lag-regression maps of rainfall with the time series of the first mode during the same period for SON, DJF, MAM and JJA are shown in Fig. 3. In SON, a positive rainfall anomaly is significant over the Indian continent and the Bay of Bengal, whereas another positive anomaly expands from the maritime continent to the eastern South Indian Ocean, which is dynamically linked to a pair of off-equatorial anomalous cyclones in the lower troposphere (not shown). According to *Kawamura et al.* [2003], such a split feature of rainfall anomaly into both hemispheres over the Indian Ocean dominates especially in late summer, associated with the growth phase of ENSO, indicating a direct ENSO impact on the South Asian summer monsoon system. A negative anomaly is zonally elongated over the central and eastern equatorial Pacific from SON to DJF. Once a warm event occurs, the anomaly disappears rapidly and conversely, an alternate anomaly develops over the same region in JJA. Likewise, a positive anomaly can be seen east of the Philippines before the onset of the warm event. In DJF, a significant positive anomaly covers northern and northeastern Australia, implying that the Australian summer monsoon is more active than normal.

Figure 4 displays the lag-regression maps of 200-hPa velocity potential with the time series of the first mode. In SON, a divergent anomaly expands from the eastern half of the tropical Indian Ocean to the maritime continent. South Asia and Australia are also covered by the divergent anomaly. In contrast, a convergent anomaly is dominant over the central and eastern tropical Pacific. These indicate a strong phase of the Walker circulation, which is quite

consistent with the anomalous rainfall pattern (Fig. 3a). Despite almost unchanged convergent anomaly over the tropical Pacific from SON to DJF, the significant divergent anomaly diminishes and is confined in the vicinity of the maritime continent. In MAM, the divergent anomaly further moves eastward into the western tropical Pacific although its magnitude becomes small, and in the meantime the convergent anomaly over the tropical Pacific disappears. In JJA after the phase transition, the Indian Ocean is covered by a new convergent anomaly, which is contrasted with SON regression pattern. A divergent anomaly is also seen over the eastern tropical Pacific, corresponding well to the growth phase of a warm event. These features indicate the frequent occurrence of the TBO-like ENSO during period I. The overall structure of this regime resembles a conceptual model of TBO proposed by *Meehl and Arblaster* [2002].

3.2 Prolonged ENSO regime

As stated earlier, prolonged ENSO occurred frequently during period II after the late 1970s. Thus, we term ENSO-related circulation features during period II prolonged ENSO regime for convenience. Figure 5 shows the lag-regression maps of SST with the time series of the first mode when this regime dominates. Comparing it with Fig. 2, there exist several distinctive differences as expected. Although the polarity of SST anomaly over the eastern tropical Pacific is reversed in MAM during period I when the TBO-like ENSO regime is prominent, the prolonged ENSO regime has a persistence of SST anomaly there from MAM to JJA. Looking at the tropical Indian Ocean, a negative SST anomaly is not necessarily obvious in fall and winter, but develops in the subsequent spring and summer, while during period I it becomes less significant from MAM to JJA. Another notable difference is the presence of a remarkable positive SST anomaly over the warm pool region of the western Pacific. The persistent positive anomaly is most evident in MAM. In contrast, there is no significant positive anomalies in the same season during period I. It should be stressed, thus, that the

seasonal evolution of SST anomalies over the tropical western North Pacific and Indian Ocean is significantly different between the two regimes as well as the eastern tropical Pacific.

As shown in Fig. 6, rainfall regression patterns during period II after the late 1970s are also obviously different from those during period I. A positive rainfall anomaly over the Philippine Sea is persistent from DJF to MAM. In the vicinity of the eastern tropical Pacific, a negative anomaly can be seen until JJA. Very interestingly, a zonally-elongated positive anomaly abruptly appears over the northern Indian Ocean in MAM, which is quite contrasted with the MAM pattern during period I. This feature is also derived from an EOF analysis for outgoing longwave radiation anomaly field over the Indian Ocean in spring [*Kajikawa et al.,* 2003] and is identified with a major precursory signal of anomalous Asian summer monsoon associated with the decay phase of ENSO [e.g., *Ju and Slingo,* 1995; *Kawamura,* 1998]. In DJF, a positive anomaly over northern and northeastern Australia is less significant than that seen during period I prior to the late 1970s, which means that after the late 1970s, the Australian summer monsoon and ENSO connection becomes weak.

Figure 7 displays the lag-regression maps of 200-hPa velocity potential with the time series of the first mode during period II. SON pattern is very similar to that observed during period I. In DJF, a more noticeable divergent anomaly develops over the Philippine Sea. A remarkable difference between the two regimes can be seen in MAM panel. The MAM pattern is not very significant during the TBO-like ENSO regime except for the western tropical Pacific. Conversely, significant areas expand in the tropics in MAM during the prolonged ENSO regime. It is found, in particular, that a divergent anomaly in the vicinity of the Philippine Sea and maritime continent extend westward into the northern Indian Ocean and South Asia in this season, which is accompanied by the positive rainfall anomaly over the Indian Ocean as indicated in Fig. 6. *Kawamura et al.* [2001a, b] pointed out that a wind-evaporation-SST (WES) feedback is frequently excited over the tropical Indian Ocean especially in spring during the decay phase of prolonged ENSO and significantly affects South

Asian monsoon activity in the subsequent summer as a delayed and indirect impact of ENSO. They also suggested that persistent anomalous convective heating in the vicinity of the Philippine Sea possibly triggers a WES mode over the tropical Indian Ocean through the westward propagation of equatorially asymmetric Rossby waves. So it appears that the above processes are, at least partially, responsible for the westward expansion of rainfall and 200-hPa divergent anomalies into the northern Indian Ocean from DJF to MAM, as seen in Figs. 6 and 7.

It turns about that there are considerable differences between the TBO-like ENSO and prolonged ENSO regimes in terms of the cross-basin connection between the tropical Indian and Pacific Oceans. It is thus meaningful to explore whether a CGCM simulation can capture either the TBO-like ENSO or prolonged ENSO regimes, which will be presented in the following section.

4. Model ENSO

As already shown in Fig. 1, the first mode in the model SST field is similar to those observed in terms of spatial and temporal patterns. In a similar fashion, the lag-regression maps of model SST with the time series of its first mode is exhibited in Fig. 8. A negative SST anomaly is prominent over the central and eastern tropical Pacific from SON to DJF, and a positive anomaly is indicated over the warm pool region of the western North Pacific. In MAM, however, the positive anomaly over the Philippine Sea disappears and another positive anomaly is established in the vicinity of the equator between 150ºE-180º. This anomaly moves eastward into the eastern equatorial Pacific from MAM to JJA, which results in the retreat of the negative anomaly there. In the Indian Ocean sector, it is seen that a negative anomaly is enhanced from SON to DJF and gradually weakens from MAM to JJA.

Figure 9 shows the lag-regression maps of model rainfall with the time series of the first mode. A north-south split feature of positive rainfall anomalies over the tropical Indian Ocean is simulated in SON and those anomalies amplify and move eastward to the maritime

continent in DJF. Such a split structure resembles that observed during period I when the TBO-like ENSO appears frequently (see Fig. 3). North-south twin circulation anomalies in the lower troposphere accompany its split structure (figure not shown). Although the twin positive anomalies dissipate in MAM, its northern counterpart is still evident and moves eastward to the central equatorial Pacific from MAM to JJA, linked with the eastward movement of the positive SST anomaly. Alternatively, a negative rainfall anomaly over the western tropical Indian Ocean expands onto the entire tropical Indian Ocean from SON to MAM. We also note here that this simulation does not capture the significant positive rainfall anomaly over the northern Indian Ocean observed in MAM during period II when the prolonged ENSO dominates, which will be discussed later.

As demonstrated in Fig. 10, model-simulated 200-hPa regression patterns indicate a regular eastward movement of anomalies from SON to JJA. In SON, a divergent anomaly is centered near the maritime continent, accompanied by two convergent anomalies over the eastern tropical Pacific and the western Indian Ocean. The divergent anomaly moves systematically eastward to the central equatorial Pacific from SON to JJA, corresponding well to the movement of the positive rainfall anomaly. Such an eastward-propagating feature is in good agreement with that observed during period I prior to the late 1970s although its phase speed is slower. Because the positive rainfall anomaly is absent over the northern Indian Ocean in MAM, as shown in Fig. 9, we cannot see any westward expansion of divergent anomalies from the warm pool region of the western North Pacific to the northern Indian Ocean which is dominant during period II after the late 1970s. Thus, the model is not expected to simulate the indirect ENSO impact on the South Asian monsoon system at its decay phase that is suggested in *Kawamura et al.* [2001a, b].

It is plausible that the regular eastward-moving features simulated in the anomalous rainfall and 200-hPa velocity potential fields are attributed to the behavior of SST anomalies in the tropics. To examine to what extent the simulated tropical SST anomalies are influenced by

ocean dynamics, we present, in Fig. 11, the lag-regression maps of model heat content with the time series of the first SST mode. Note that the heat content is vertically integrated from surface to a depth of 300 m. In the tropical Pacific, a positive anomaly is concentrated to the east of the Philippines in SON and it moves eastward along the equator from DJF to JJA. In DJF, a pronounced anomalous cyclone can be seen over the Philippine Sea and it looks like that the associated westerly anomaly induces the equatorward and eastward movement of the positive heat content anomaly (not shown). Looking at Fig. 12, showing the longitude-depth sections of subsurface temperature regression patterns along the equator, a positive subsurface temperature anomaly in the warm pool region of the western Pacific moves eastward along the equator from SON to JJA, which is a signature of eastward-propagating downwelling Kelvin waves. Because the phase speed of the simulated Kelvin waves is slower than that of internal Kelvin waves, those waves may cross the equatorial Pacific as an air-sea coupled mode [e.g., Zhang and Levitus, 1997; *Iizuka et al.,* 2003]. It is found that the positive SST anomaly over the equatorial Pacific moves eastward from MAM to JJA, linked with the eastward propagation of the equatorial Kelvin waves. It is thus inferred that in this simulation, the SST-thermocline feedback [*Philander et al.,* 1984] strongly controls the time evolution of SST anomalies over the equatorial Pacific.

In the tropical Indian Ocean, zonally asymmetric anomalies between its western and eastern parts are simulated in the heat content field from SON to DJF, but this structure disappears in MAM. Conversely, a reversed zonally asymmetric pattern is established in JJA. Looking at Fig. 12 again, from SON to DJF a salient positive subsurface temperature anomaly is indicated in the eastern equatorial Indian Ocean and a negative anomaly is located in its western counterpart. In contrast, an alternated pattern is organized in JJA. These features may reflect the dominance of westward-propagating downwelling Rossby waves. An intriguing feature in the tropical Indian Ocean is that an apparent zonally asymmetric pattern of anomalous heat content from SON to DJF cannot be seen in the SST anomaly filed. This may

suggest that the influential role of ocean dynamics in the tropical Indian Ocean SSTs is less important than that in the tropical Pacific so far as the model ENSO-related anomalies are concerned, although we are aware, of course, that several recent studies emphasize a substantial role of the ocean dynamics in generating the tropical Indian Ocean SST anomalies [e.g., *Saji et al.*, 1999; *Webster et al.*, 1999; *Iizuka et al.*, 2000; *Rao et al.*, 2002; *Xie et al.*, 2002]. The role of surface heat flux in model SST anomalies over the Indian Ocean outside of the equatorial waveguide may become relatively important [e.g., *Yu and Rienecker*, 1999; *Lau and Nath*, 2000; 2003]. *Kawamura et al.* [2003] suggested that a combination of the wind-evaporation feedback in the Indian Ocean and ocean dynamics in the tropical Pacific is prerequisites for the phase transition of the anomalous Walker circulation system over the two oceans associated with the TBO-like ENSO. It is quite possible that the CGCM simulation captures such dynamic processes.

5. Discussion

5.1 A contribution of westerly wind bursts to ENSO onset

In the previous section, it is noted that there are some similarities and discrepancies between model results and observations in terms of the lag-regression analysis on a seasonal basis. As for the TBO-like ENSO regime, one of the similarities is the systematic eastward movement of the anomalous rainfall and 200-hPa velocitiy potential from the Indian Ocean sector to the tropical Pacific sector. It is expected that with this eastward movement, a low-level westerly anomaly, accompanied by enhanced rainfall, intrudes into the western tropical Pacific and an anomalous easterly over the tropical Pacific region retreats eastward, being an important trigger of downwelling equatorial Kelvin waves propagating eastward along the equator [e.g., *Masumoto and Yamagata*, 1991; *Moore and Kleeman*, 1999]. A pair of off-equatorial anomalous cyclones accompanies the low-level westerly anomaly over the western equatorial during the mature phase of a cold event. However, it looks like that its

origin comes from the tropical Indian Ocean, as *Barnett* [1983; 1984] and *Yasunari* [1985; 1990; 1991] already pointed out, which may not be consistent with other ENSO paradigms that do not necessarily require the role of the Indian Ocean. It is thus meaningful to examine how an onset of model ENSO occurs to confirm the above process.

Figure 13 shows the behavior of an onset of model El Nino that occurred in the summer of the 18th year as a typical case. Left panel is the time-longitude section of 5-day mean heat content and zonal wind stress anomalies along the equator, and right panel is that of 5-day mean SST and rainfall anomalies. Positive rainfall anomalies are located over the eastern Pacific and Indian Ocean from January 17th year to April 17th year, indicating the persistence of a warm event. After that, a negative SST anomaly expands into the Pacific region east of 150ºE, accompanied by a negative rainfall anomaly, whereas over the Indian Ocean the positive rainfall anomaly is still sustained. This implies the prominence of a cold event and its state continues until the end of the 17th year. Over the Indian Ocean, a negative SST anomaly is established in its western part around October 17th year and extends eastward by January 18th year. Associated with this, the positive rainfall anomaly rapidly shifts in February or March 18th year from the Indian Ocean to the western Pacific. With the eastward shift of the rainfall anomaly, a group of westerly wind stress anomalies start to intrude into the warm pool region of the western Pacific. When strong westerly bursts occur over its warm pool region in May 18th year, an outstanding positive heat content anomaly propagates eastward to the central and eastern Pacific. Its phase speed is about 1.5 m s^{-1}, which is comparable to that of an internal Kelvin wave. Corresponding to the eastward propagation of the anomalous heat content, a positive SST anomaly also shifts from the western Pacific to the central Pacific and maintains after June 18th year. The positive rainfall anomaly further shifts eastward and is maintained over the central Pacific. These features indicate the onset phase of a warm event. The positive SST anomaly over the Pacific sector further expands, and we see two positive

rainfall anomalies over the two ocean basins again from October 18th year, implying the mature phase of the warm event.

It is thus recognized that westerly wind bursts contribute substantially to the onset of a model warm event. Occurrence of the westerly wind bursts is not independent of the phase transition of anomalous Walker circulation over the two ocean basins. Its phase transition provides a favorable condition for inducing the westerly wind bursts over the warm pool region of the western Pacific. It should also be emphasized here that the cross-basin connection between the tropical Indian and Pacific Oceans is important for the turnabout of model ENSO as an additional dynamic process, although we do not disregard the previous ENSO theories. *Kawamura et al.* [2003] demonstrated that the TBO-like regime has four stages: i.e., onset and mature phases of a cold event, and onset and mature phases of a warm event, which will be termed phase I, II, III and IV, respectively, for convenience. If this classification is applied to Fig. 13, the period from January 17th year to April 17th year corresponds to phase IV. Phase I, which is characterized by an ascending branch over the Indian Ocean and a descending branch over the central and eastern Pacific, continues until the end of the 17th year, with an anomalous east-west SST gradient between the two ocean basins. They also pointed out that the SST decrease over the Indian Ocean and the associated localization of enhanced rainfall over the warm pool region of the western Pacific result in the transition from phase I to II. It looks like that the model simulates such a process. At phase II, along with an ascending branch over the maritime continent and two descending branches over the Indian Ocean and the central and eastern Pacific, westerly bursts begin to dominate over its warm pool, eventually bringing about the onset of a model warm event (phase III). Although only a typical case is presented in this figure, similar features can also be seen in other events (figure not shown).

We note, on the other hand, that there are also discrepancies between model results and observations. If the TBO-like ENSO regime is highlighted again, one of the discrepancies is the presence of a significant model SST anomaly around the equator between 150ºE-180º in

MAM. In observations, there are no significant positive anomalies over that region, as seen in Fig. 2c. According to *Iizuka et al.* [2003], the model used in this study has a systematic error that the mean thermocline depth in the western equatorial Pacific is shallower than that observed. Thus, model SST anomalies over the western equatorial Pacific are expected to be too sensitive to ocean dynamics, compared to observations. This systematic error might produce the difference in periodicity between the model ENSO and observed TBO-like ENSO.

5.2 Why can't the model simulate the prolonged ENSO regime observed?

As mentioned before, the model does not simulate any westward expansion of rainfall and upper-level divergent anomalies from the warm pool region of the western North Pacific to the northern Indian Ocean that is frequently observed in MAM during period II after the late 1970s. As for period II, there is also a clear difference in MAM SST between model results and observations. Although an apparent positive SST anomaly is observed over the warm pool region east of the Philippines, the model anomaly is confined to the equator between 150ºE-180º due to the above-mentioned systematic error. According to *Wang et al.* [2000], the observed anomaly is generated both by in situ air-sea interaction and by remote forcing. The model rainfall anomaly also tends to expand toward the equator. So it is quite possible that the difference in convective heating distribution over the tropical western Pacific influences the excitation of a WES mode over the tropical Indian Ocean. If the model SST over the western equatorial Pacific is not sensitive to ocean dynamics, it is also conceivable to produce a significant SST anomaly over the Philippine Sea through Wang et al's processes, which might result in establishing similar dynamic structures to the observed prolonged ENSO. Unfortunately, this is beyond of the scope of this study.

In observations, the positive SST anomaly over the Philippine Sea in DJF and MAM is more evident during the prolonged ENSO regime than during the TBO-like ENSO regime (see Figs. 2 and 5). This anomaly contributes to form an anomalous meridional SST gradient

between the Philippine Sea and the Timor and Arafra Sea, which facilitates the generation of equatorially asymmetric convective heating anomalies in the vicinity of the maritime continent. The equatorially asymmetric convective heating can trigger a WES mode over the tropical Indian Ocean from DJF to MAM, and conversely, is not very likely to produce a favorable condition for the frequent occurrence of westerly wind bursts over the western equatorial Pacific because low-level westerly anomalies are enhanced away from the equator due to the Rossy wave response to the equatorially asymmetric convective heating. The absence of strong westerly wind bursts may lead to the continuation of a cold event of ENSO. If so, the periodicity of ENSO might shift toward longer timescales. It still remains, however, why the SST anomaly distributions over the western tropical Pacific in DJF and MAM are apparently different between the TBO-like ENSO and prolonged ENSO regimes. Further clarification should be required.

6. Summary

To understand two different regimes of anomalous Walker circulation over the Pacific and Indian Oceans before and after the late 1970s, we investigated the seasonal evolutions of the two regimes in terms of cross-basin connection, using the NCEP/NCAR reanalysis aided by a coupled ocean-atmosphere model. Considering the climate shift in the late 1970s, we focused specifically on two 15-yr periods before and after the late 1970s: i.e., the former and latter periods are termed tropospheric biennial oscillation (TBO)-like ENSO and prolonged ENSO regimes, respectively.

In the TBO-like ENSO regime, it is characteristic that anomalous rainfall and 200-hPa velocitiy potential systematically move eastward from the tropical Indian Ocean to the warm pool region of the western Pacific during the growth phase of ENSO. In the meantime, the activities of South Asian and Australian summer monsoon systems are directly influenced by the evolution of the anomalous Walker circulation. When a cold event develops, a low-level

westerly anomaly, accompanied by enhanced rainfall, intrudes into the warm pool region of the western Pacific. The model used in this study is successful in simulating the basic features of such systematic eastward movement. It is found that westerly wind bursts over its warm pool, which depend on the phase transition of the anomalous Walker circulation over the two ocean basins, contribute substantially to the onset of model warm event through the excitation of downwelling equatorial Kelvin waves. It is thus suggested that the cross-basin connection is prerequisites for the turnabout of the TBO-like ENSO as an additional dynamic process.

In the prolonged ENSO regime, on the other hand, it is characteristic that a 200-hPa velocitiy potential anomaly in the vicinity of the Philippine Sea and maritime continent extend westward into the northern Indian Ocean and South Asia during the decay phase of ENSO, which is accompanied by an apparent rainfall anomaly over the Indian Ocean. This westward expansion is identified with a major precursory signal of anomalous South Asian summer monsoon related to the decay phase of ENSO, which is, at least partially, a manifestation of a positive wind-evaporation-SST (WES) feedback prevailing in spring over the tropical Indian Ocean. However, the model cannot capture such westward expansion. One of the reasons may be the absence of a noticeable SST anomaly in spring over the Philippine Sea away from the equator because the excitation of a WES mode requires the persistence of equatorially asymmetric convective heating anomalies around the maritime continent. Due to a systematic error of the model, it appears that model SST anomalies over the western equatorial Pacific are too sensitive to ocean dynamics, compared to observations. As a consequence, the model ENSO is relatively similar to the TBO-like ENSO, in terms of spatial structures, that requires the systematic occurrence of westerly wind bursts over the western equatorial Pacific, but it is different from the prolonged ENSO that requires the pronounced SST anomaly over the Philippine Sea away from the equator at its decay phase, even though its periodicity is similar to each other.

New findings obtained in this study suggest that the cross-basin connection between the tropical Indian and Pacific Oceans is apparently different between the two regimes of anomalous Walker circulation before and after the late 1970s. This difference is very likely to bring about the controversial results on the lag relationship between the South Asian summer monsoon and ENSO, and might also be one of the possible reasons why the changes in ENSO properties occurred around the late 1970s. An alternated hypothesis is that the Pacific climate shift causes the decadal changes of ENSO properties [e.g., *Wang and An*, 2002]. We need further intensive investigation on the dynamic and thermodynamic processes of large-scale air-sea interaction in the western tropical Pacific, linked with those in the Indian Ocean and the eastern tropical Pacific.

Acknowledgments. This research was supported by the National Research Institute for Earth Science and Disaster Prevention; by the Mitsubishi Foundation for the Promotion of Science; and by Grants-in-Aids (14540406) of the Japanese Ministry of Education, Sports, Culture, Science and Technology.

References

Angell, J. K., Comparison of variations in atmospheric quantities with sea surface temperature variations in the equatorial eastern Pacific, *Mon. Wea. Rev.*, **109**, 230-243, 1981.

Arakawa, A., and W. H. Schubert, Interaction of a cumulus cloud ensemble with the large-scale environment. Part I, *J. Atmos. Sci.*, **31**, 674-701, 1974.

Ashok, K., Z. Guan, and T. Yamagata, Impact of the Indian Ocean dipole on the relationship between the Indian monsoon rainfall and ENSO, *Geophys. Res. Lett.*, **28**, 4499-4502, 2001.

Barnett, T. P., Interaction of the monsoon and Pacific trade wind systems at interannual time

scales. Part I: The equatorial zone, *Mon. Wea. Rev.*, **111**, 756-773, 1983.

Barnett, T. P., Interaction of the monsoon and Pacific trade wind system at interannual time scale. Part III: A partial anatomy of the Southern Oscillation, *Mon. Wea. Rev.*, **112**, 2388-2400, 1984.

Chang, C.-P., P. Harr, and J. Ju, Possible roles of Atlantic circulations on the weakening Indian monsoon rainfall-ENSO relationship, *J. Clim.*, **14**, 2376-2380, 2001.

Chen, T.-C., and M.-C. Yen, Interannual variation of the Indian monsoon simulated by the NCAR community climate model: Effect of the tropical Pacific SST. *J. Clim.,* **7**, 1403-1415, 1994.

Iizuka, S., T. Matsuura, and T. Yamagata, The Indian Ocean SST dipole simulated in a coupled general circulation model, *Geophys. Res. Lett.*, **27**, 3369-3372, 2000.

Iizuka, S., K. Orito, T. Matsuura, and M. Chiba, Influence of cumulus convection schemes on the ENSO-like phenomena simulated in a CGCM, *J. Meteorol. Soc. Jpn*, **81**, in press, 2003.

Jin, F. F., An equatorial ocean recharge paradigm for ENSO. Part I: Conceptual model, *J. Atmos. Sci.*, **54**, 811-829, 1997.

Ju, J., and J. M. Slingo, The Asian summer monsoon and ENSO, *Quart. J. Roy. Meteor. Soc.*, **121**, 1133-1168, 1995.

Kajikawa, Y., T. Yasunari, and R. Kawamura, The role of the local Hadley circulation over the

western Pacific on the zonally asymmetric anomalies over the Indian Ocean, *J. Meteorol. Soc. Jpn*, **81**, in press, 2003.

Kalnay, E., and Coauthors, The NCEP/NCAR 40-year reanalysis project, *Bull. Amer. Meteorol. Soc.*, **77**, 437-471, 1996.

Kawamura, R., A possible mechanism of the Asian summer monsoon-ENSO coupling, *J. Meteorol. Soc. Jpn*, **76**, 1009-1027, 1998.

Kawamura, R., M. Sugi, T. Kayahara, and N. Sato, Recent extraordinary cool and hot summers in East Asia simulated by an ensemble climate experiment, *J. Meteorol. Soc. Jpn*, **76**, 597-617, 1998.

Kawamura, R., T. Matsuura, and S. Iizuka, Role of equatorially asymmetric sea surface temperature anomalies in the Indian Ocean in the Asian summer monsoon and El Nino-Southern Oscillation coupling, *J. Geophys. Res*., **106**, 4681-4693, 2001a.

Kawamura, R., T. Matsuura, and S. Iizuka, Interannual atmosphere-ocean variations in the tropical western North Pacific relevant to the Asian summer monsoon-ENSO coupling, *J. Meteorol. Soc. Jpn*, **79**, 883-898, 2001b.

Kawamura, R., T. Matsuura, and S. Iizuka, Equatorially symmetric impact of El Nino-Southern Oscillation on the South Asian summer monsoon system, *J. Meteorol. Soc. Jpn*, **81**, in press, 2003.

Kinter, J. L., K. Miyakoda, and S. Yang, Recent change in the connection from the Asian monsoon to ENSO, *J. Clim.,* **15**, 1203-1215, 2002.

Krishnamurthy, V., and B. N. Goswami, Indian monsoon-ENSO relationship on interdecadal timescale, *J. Clim.,* **13**, 579-595, 2000.

Kuma, K., Parameterization of cumulus convection, *JMA/NPD Report,* No. 42, 93pp, 1996.

Kumar, K. K., B. Rajagopalan, and M. A. Cane, On the weakening relationship between the Indian monsoon and ENSO, *Science*, **284**, 2156-2159, 1999.

Lau, K.-M., and H. T. Wu, Principal modes of rainfall-SST variability of the Asian summer monsoon: A reassessment of the monsoon-ENSO relationship, *J. Clim.*, **14**, 2880-2895, 2001.

Lau, N.-C., and M. J. Nath, Impacts of ENSO on the variability of the Asian-Australian monsoons as simulated in GCM experiments, *J. Clim.*, **13**, 4287-4309, 2000.

Lau, N.-C., and M. J. Nath, Atmosphere-ocean variations in the Indo-Pacific sector during ENSO episodes, *J. Clim.*, **16**, 3-20, 2003.

Levitus, S., Climatological atlas of the world ocean, *NOAA Prof. Paper 13*, 178pp., Natl. Oceanic and Atmos. Admin., Silver Spring, Md., 1982.

Li, T., and Y. Zhang, Processes that determine the quasi-biennial and lower-frequency variability of the South Asian monsoon, *J. Meteor. Soc. Japan*, **80**, 1149-1163, 2002.

Masumoto, Y., and T. Yamagata, On the origin of a model ENSO in the western Pacific, *J. Meteorol. Soc. Jpn*, **69**, 197-207, 1991.

Meehl, G. A., The annual cycle and interannual variability in the tropical Pacific and Indian Ocean regions, *Mon.Wea. Rev.*, **115**, 27-50, 1987.

Meehl, G. A., A coupled air-sea biennial mechanism in the tropical Indian and Pacific regions: Role of the ocean, *J. Clim.*, **6**, 31-41, 1993.

Meehl, G. A., and J. M. Arblaster, The tropospheric biennial oscillation and Asian-Australian monsoon rainfall, *J. Clim.*, **15**, 722-744, 2002.

Mitchell, T. P., and J. M. Wallace, ENSO seasonality: 1950-78 versus 1979-92, *J. Clim.*, **9**, 3149-3161, 1996.

Miyakoda, K., J. L. Kinter, and S. Yang, Analysis of the connection from the South Asian monsoon to ENSO by using precipitation and circulation indices, *COLA Technical Report*, **90**, Center for Ocean-Land-Atmosphere Studies, 72pp., 2000.

Moore, A. M., and R. Kleeman, Stochastic forcing of ENSO by the intraseasonal oscillation, *J. Clim.*, **12**, 1199-1220, 1999.

Murakami, T., and J. Matsumoto, Summer monsoon over the Asian continent and western North Pacific, *J. Meteorol. Soc. Jpn,* **72**, 719-745, 1994.

Pacanowski, R. C., Documentation user's guide and reference manual (MOM2, Version 2), *GFDL Ocean Technical Report 3.2*, 329pp, Geophys. Fluid Dyn. Lab., Princeton, N. J., 1996.

Pacanowski, R. C., and S. G. H. Philander, Parameterization of vertical mixing in numerical

models of tropical oceans, *J. Phys. Oceanogr.,* **11**, 1443-1451, 1981.

Parker, D. E., C. K. Folland, and M. Jackson, Marine surface temperature: Observed variations and data requirements, *Clim. Change*, **31**, 559-600, 1995.

Philander, S. G. H., T. Yamagata, and R. C. Pacanowski, Unstable air-sea interactions in the tropics, *J. Atmos. Sci.,* **41**, 603-613, 1984.

Rao, S. A., S. K. Behera, Y. Masumoto, and T. Yamagata, Interannual subsurface variability in the tropical Indian Ocean with a special emphasis on the Indian Ocean dipole. *Deep-Sea Res.,* **49B**, 1549-1572, 2002.

Rasmusson, E. M., and T. H. Carpenter, Variations in tropical sea surface temperature and surface wind fields associated with the Southern Oscillation/El Nino, *Mon. Wea. Rev.*, **110**, 354-384, 1982.

Rasmusson, E. M., and T. H. Carpenter, The relationship between eastern equatorial Pacific sea surface temperatures and rainfall over India and Sri Lanka, *Mon. Wea. Rev.*, **111**, 517-528, 1983.

Saji, N. H., B. N. Goswami, P. N. Vinayachandran and T. Yamagata, A dipole mode in the tropical Indian Ocean, *Nature*, **401**, 360-363, 1999.

Schopf, P. S., and M. J. Suarez, Vacillations in a coupled ocean-atmosphere model, *J. Atmos. Sci.*, **45**, 549-566, 1988.

Shen, X., M. Kimoto, and A. Sumi, Role of land surface processes associated with interannual variability of broad-scale Asian summer monsoon as simulated by the CCSR/NIES AGCM, *J. Meteorol. Soc. Jpn*, **76**, 217-236, 1998.

Shukla, J., and D. A. Paolino, The Southern Oscillation and long-range forecasting of the summer monsoon rainfall over India, *Mon. Weather Rev.,* **111**, 1830-1837, 1983.

Sugi, M., K. Kuma, K. Tada, K. Tamiya, N. Hasegawa, T. Iwasaki, S. Yamada, and T. Kitade,

Description and performance of the JMA operational global spectral model

(JMA-GSM88), *Geophys. Mag.*, **43**, 105-130, 1990.

Torrence, C., and P. J. Webster, Interdecadal changes in the ENSO-monsoon system, *J. Clim.,* **12**, 2679-2690, 1999.

Wang, B., Interdecadal changes in El Nino onset in the last four decades, *J. Clim.,* **8**, 267-285, 1995.

Wang, B., R. Wu, and X. Fu, Pacific-East Asian teleconnection: How does ENSO affect East Asian climate?, *J. Clim.,* **13**, 1517-1536, 2000.

Wang, B., R. Wu, K.-M. Lau, Interannual variability of the Asian summer monsoon: Contrasts

between the Indian and the western North Pacific-East Asian monsoons, *J. Clim.*, **14**, 4073-4090, 2001.

Wang, B., and S. I. An, A mechanism for decadal changes of ENSO behavior: roles of background wind changes, *Clim. Dyn.*, 18, 475-486, 2002.

Weisberg, R., and C. Wang, A western Pacific oscillator paradigm for the El Nino-Southern Oscillation, *Geophys. Res. Lett.*, **24**, 779-782, 1997.

Webster, P. J., and S. Yang, Monsoon and ENSO: selectively interactive systems, *Q. J. R. Meteorol. Soc.*, **118**, 877-926, 1992.

Webster, P. J., V. O. Magana, T. N., Palmer, J. Shukla, R. A. Tomas, M. Yanai, and T. Yasunari, Monsoons: Processes, predictability, and prospects for prediction, *J. Geophys. Res.*, **103**, 14451-14510, 1998.

Webster, P. J., A. M. Moore, J. P. Loschnigg, and R. R. Leben, Coupled ocean-atmospheric dynamics in the Indian Ocean during 1997-1998, *Nature,* **401**, 356-360, 1999.

Wu, R., and B. Wang, A Contrast of the East Asian Summer Monsoon and ENSO Relationship between 1962-1977 and 1978-1993, *J. Clim.,* 15, 3266-3279, 2002.

Xie, S.-P., Structure and mechanisms of South Indian Ocean climate variability, *J. Clim.*, **15**, 864-878, 2002.

Yang, S., K.-M. Lau, and M. Sankar-Rao, Precursory signals associated with the interannual variability of the Asian summer monsoon, *J. Clim.*, **9**, 949-964, 1996.

Yang, S., and K.-M. Lau, Influences of sea surface temperature and ground wetness on Asian summer monsoon, *J. Clim.*, **11**, 3230-3246, 1998.

Yasunari, T., Zonally propagating modes of the global east-west circulation associated with the Southern Oscillation, *J. Meteorol. Soc. Jpn*, **63**, 1013-1029, 1985.

Yasunari, T., Impact of Indian monsoon on the coupled atmosphere ocean system in the tropical Pacific, *Meteorol. Atmos. Phys.*, **44**, 29-41, 1990.

Yasunari, T., The monsoon year – A new concept of the climate year in the tropics, *Bull. Amer. Meteorol. Soc.*, **72**, 1331-1338, 1991.

Yu, L., and M. M. Rienecker, Mechanisms for the Indian Ocean warming during the 1997-1998 El Nino, *Geophys. Res. Lett.*, **26**, 735-738, 1999.

Zhang, R.-H., and S. Levitus, Interannual variability of the coupled tropical Pacific Ocean-Atmosphere system associated with the El Nino-Southern Oscillation, *J. Clim*, **10**, 1312-1330, 1997.

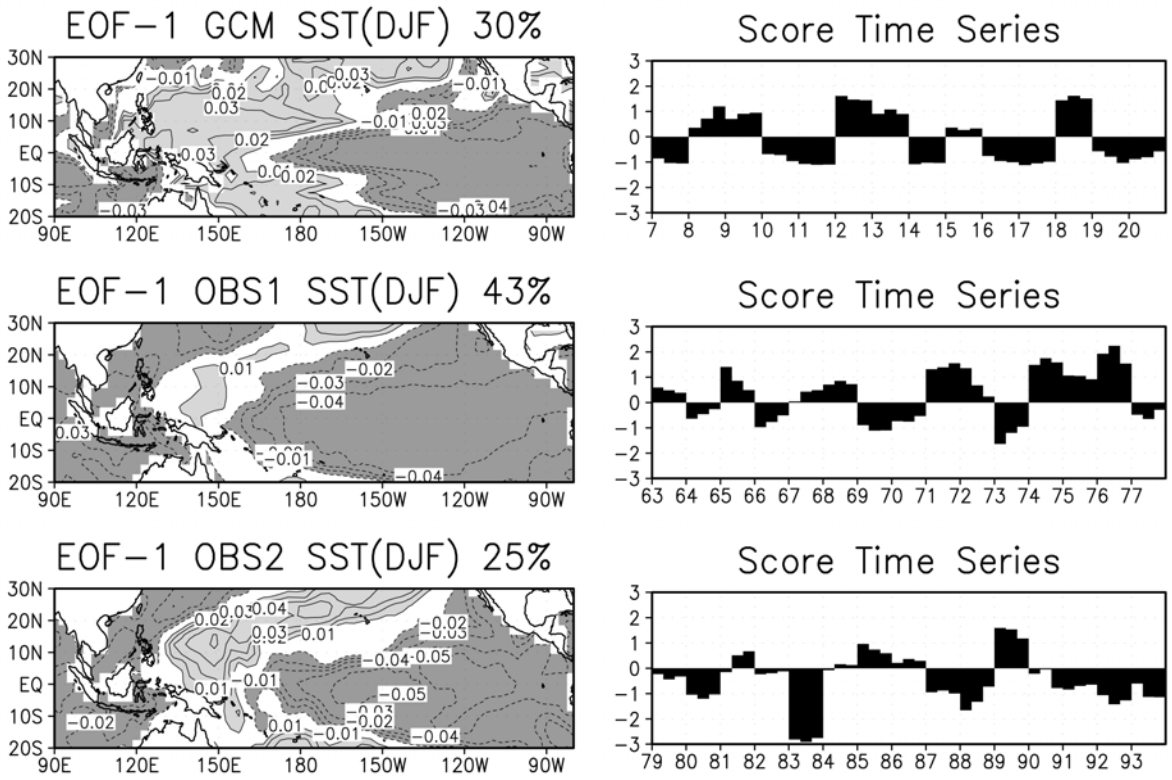

Fig. 1　Spatial patterns and time series of the first SST modes prevailing in the tropical Pacific Ocean during northern winter (December-January) for period I (1962-1976) and II (1979-1993), which are obtained from the application of a simple EOF analysis to monthly SST anomaly data.　Also denoted are those of model SST.

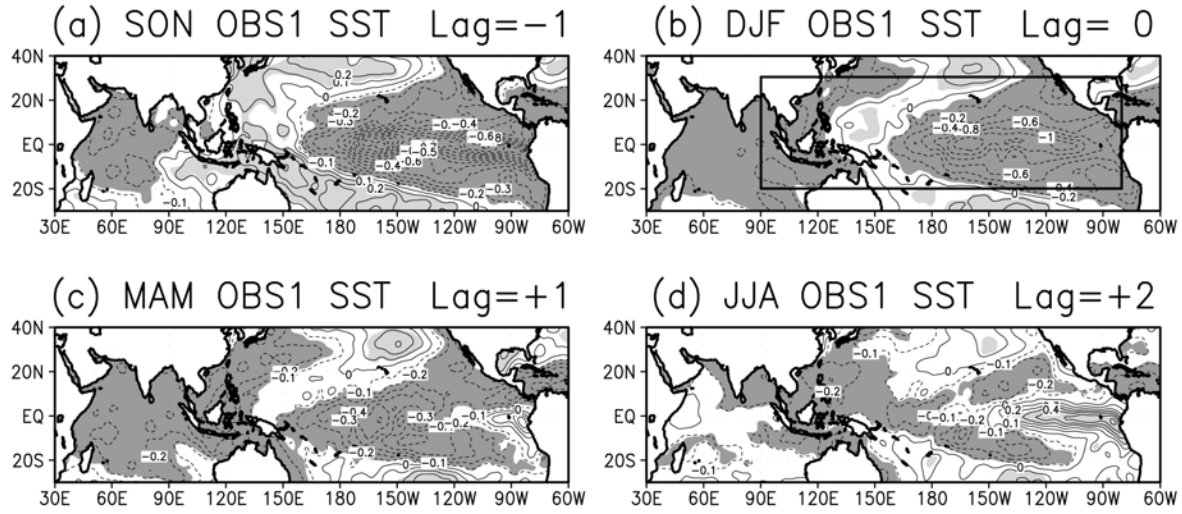

Fig. 2 Lag-regression maps of SST with the time series of the first SST mode during period I (1962-1976) for September-November (lag-1), December-February (lag0), March-May (lag+1), and June-August (lag+2). Contour interval of the regression coefficients is 0.1ºC. Shading indicates the regions where values satisfy the 5% level of statistical significance using a Student's *t*-test.

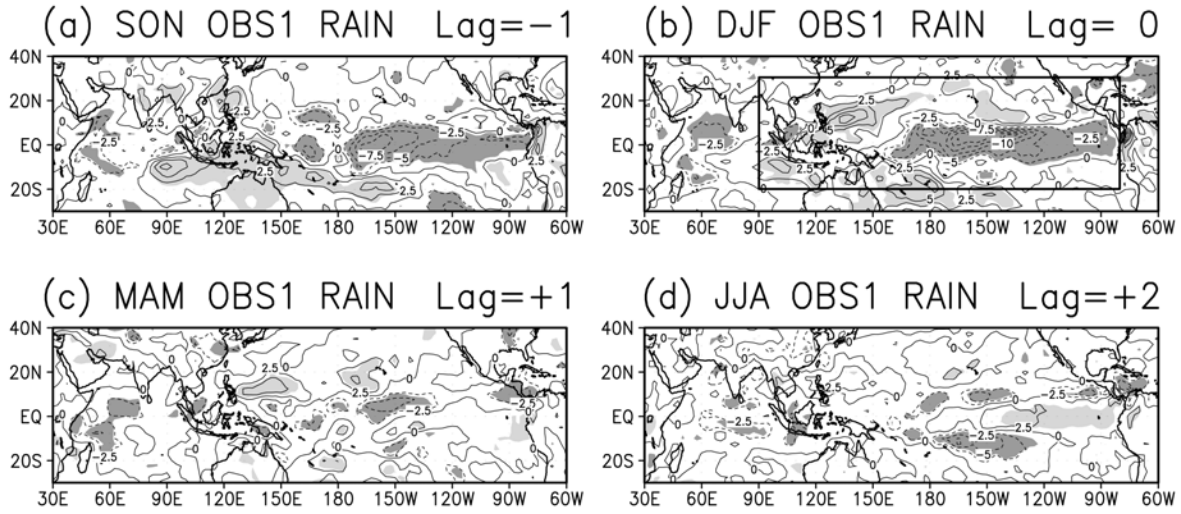

Fig. 3 As in Fig. 2 but for rainfall during period I. Contour interval is 2.5 mm day^{-1}.

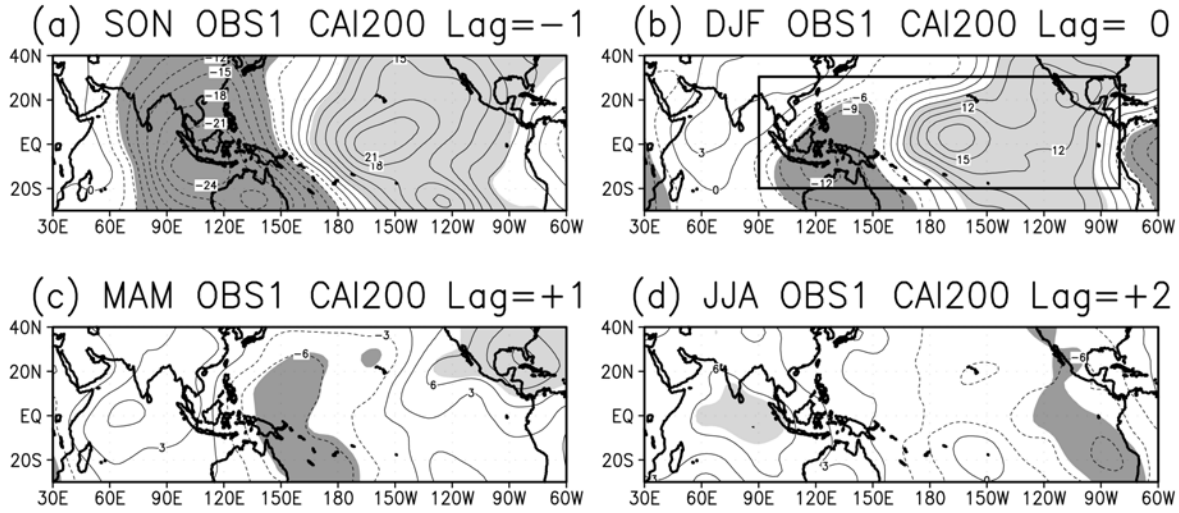

Fig. 4 As in Fig. 2 but for 200-hPa velocity potential during period I. Contour interval is 3×10^5 m^2 s^{-1}. Positive and negative anomalies denote convergent and divergent ones, respectively.

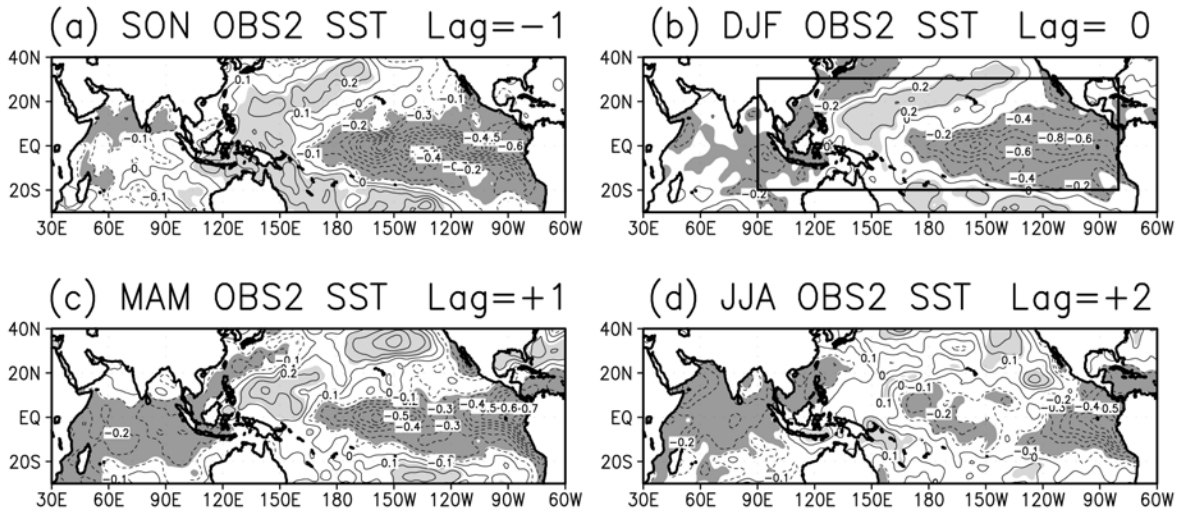

Fig. 5 Lag-regression maps of SST with the time series of the first SST mode during period II (1979-1993) for September-November (lag-1), December-February (lag0), March-May (lag+1), and June-August (lag+2). Contour interval of the regression coefficients is 0.1ºC. Shading indicates the regions where values satisfy the 5% level of statistical significance using a Student's *t*-test.

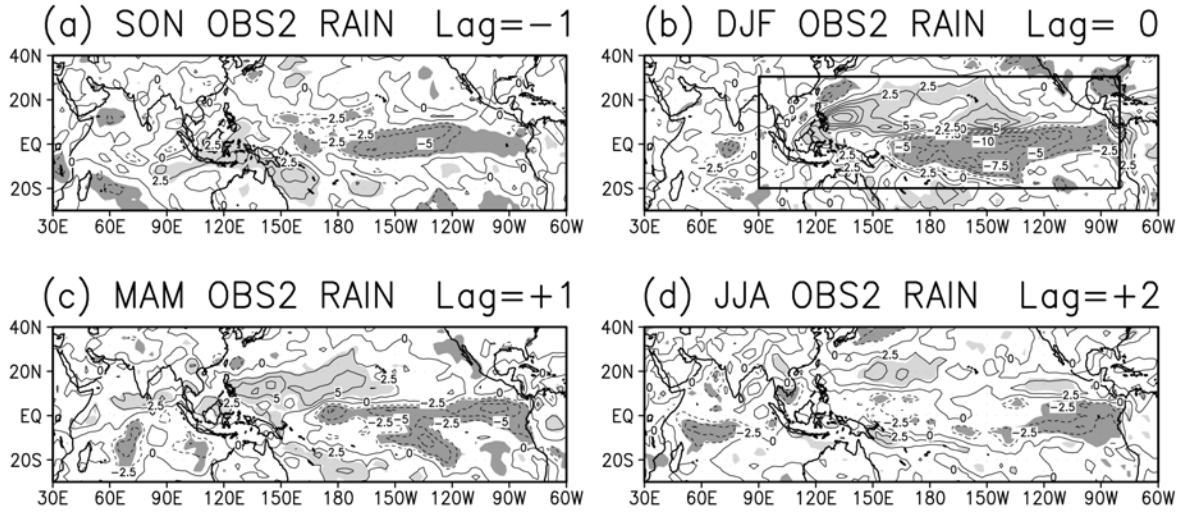

Fig. 6 As in Fig. 5 but for rainfall during period II. Contour interval is 2.5 mm day^{-1}.

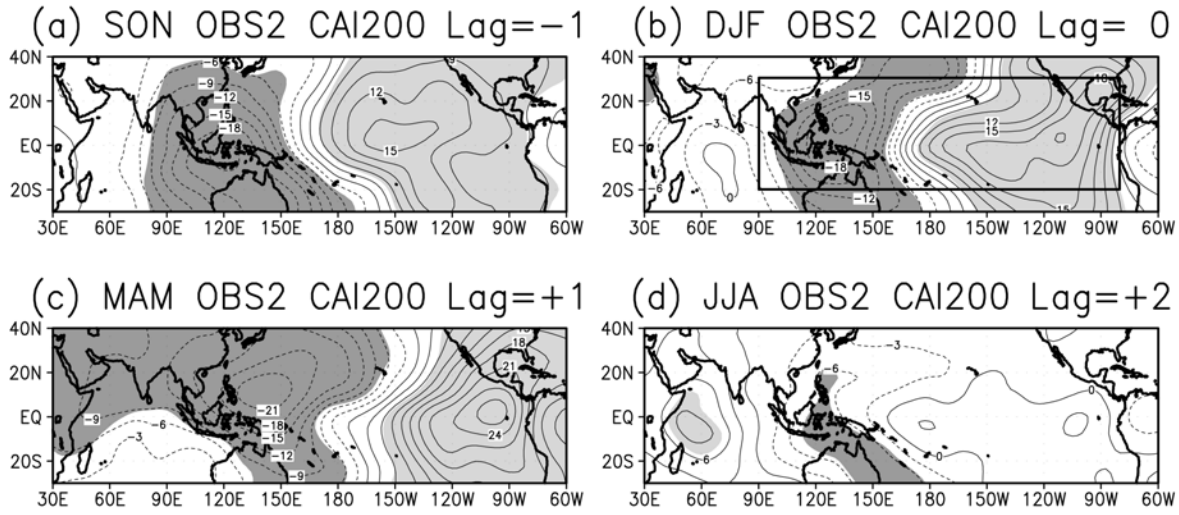

Fig. 7 As in Fig. 5 but for 200-hPa velocity potential during period II. Contour interval is 3×10^5 m^2 s^{-1}. Positive and negative anomalies denote convergent and divergent ones, respectively.

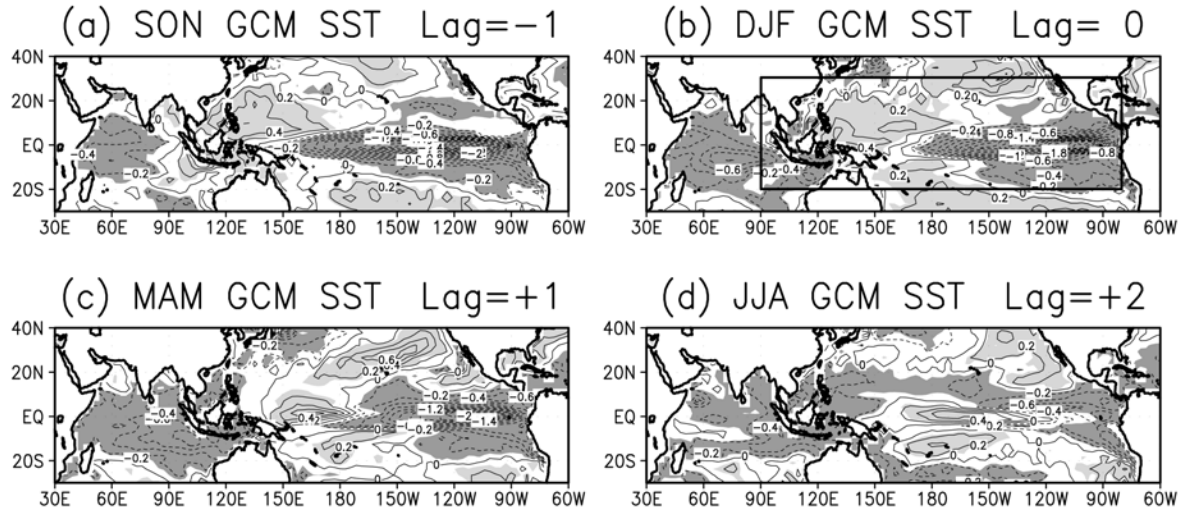

Fig. 8 Lag-regression maps of SST with the time series of the first SST mode in the model simulation for September-November (lag-1), December-February (lag0), March-May (lag+1), and June-August (lag+2). Contour interval of the regression coefficients is 0.2ºC. Shading indicates the regions where values satisfy the 5% level of statistical significance using a Student's *t*-test.

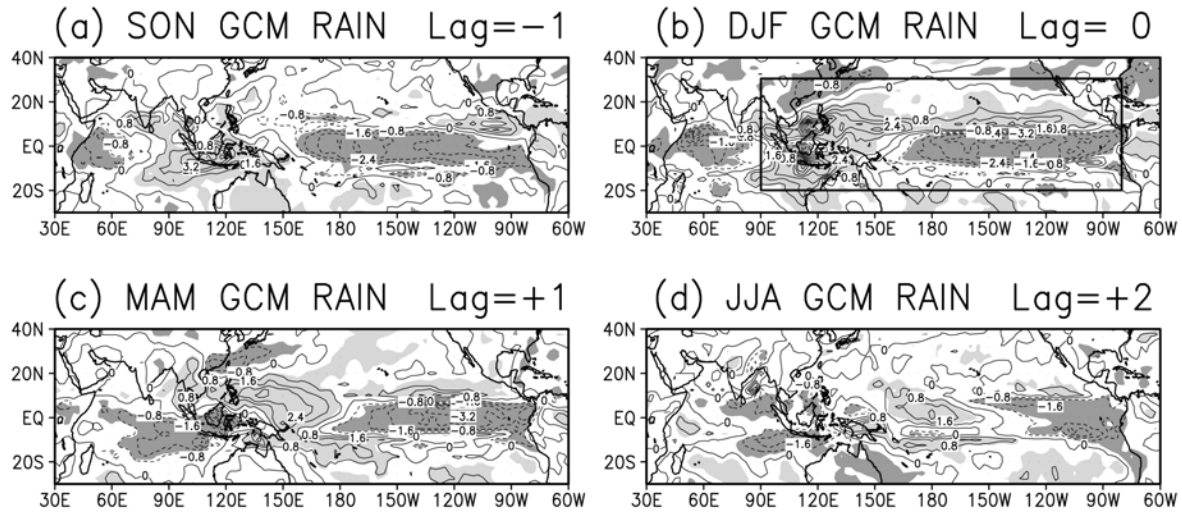

Fig. 9 As in Fig. 8 but for model rainfall. Contour interval is 0.8 mm day^{-1}.

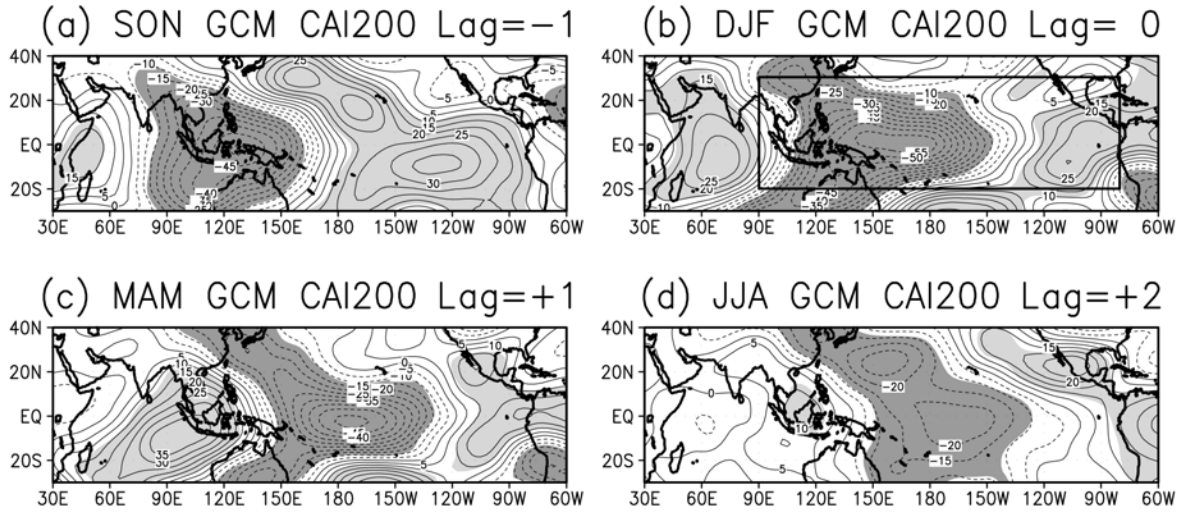

Fig. 10 As in Fig. 8 but for model-simulated 200-hPa velocity potential. Contour interval is 5×10^5 m^2 s^{-1}. Positive and negative anomalies denote convergent and divergent ones, respectively.

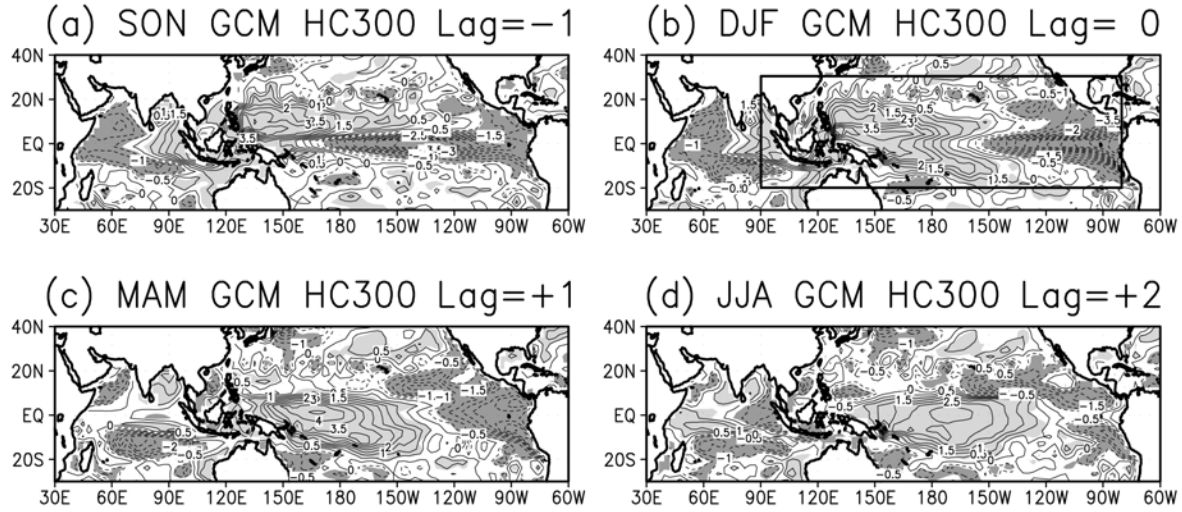

Fig. 11 As in Fig. 8 but for model heat content. Contour interval is 0.5×10^4 ºC cm.

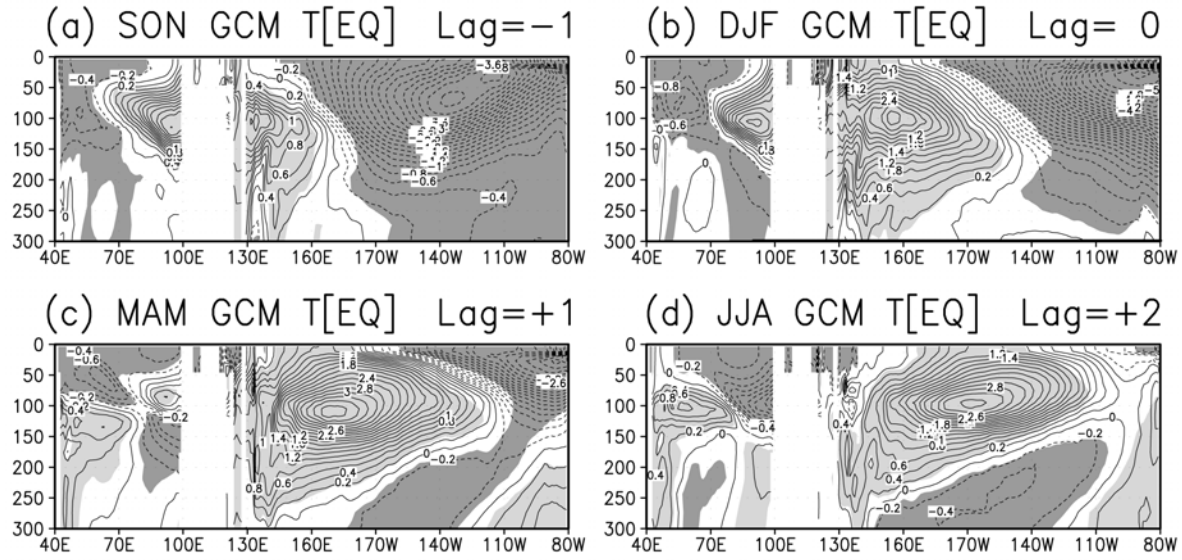

Fig. 12 As in Fig. 8 but for the depth-longitude section of model subsurface temperature along the equator. Contour interval is 0.2ºC.

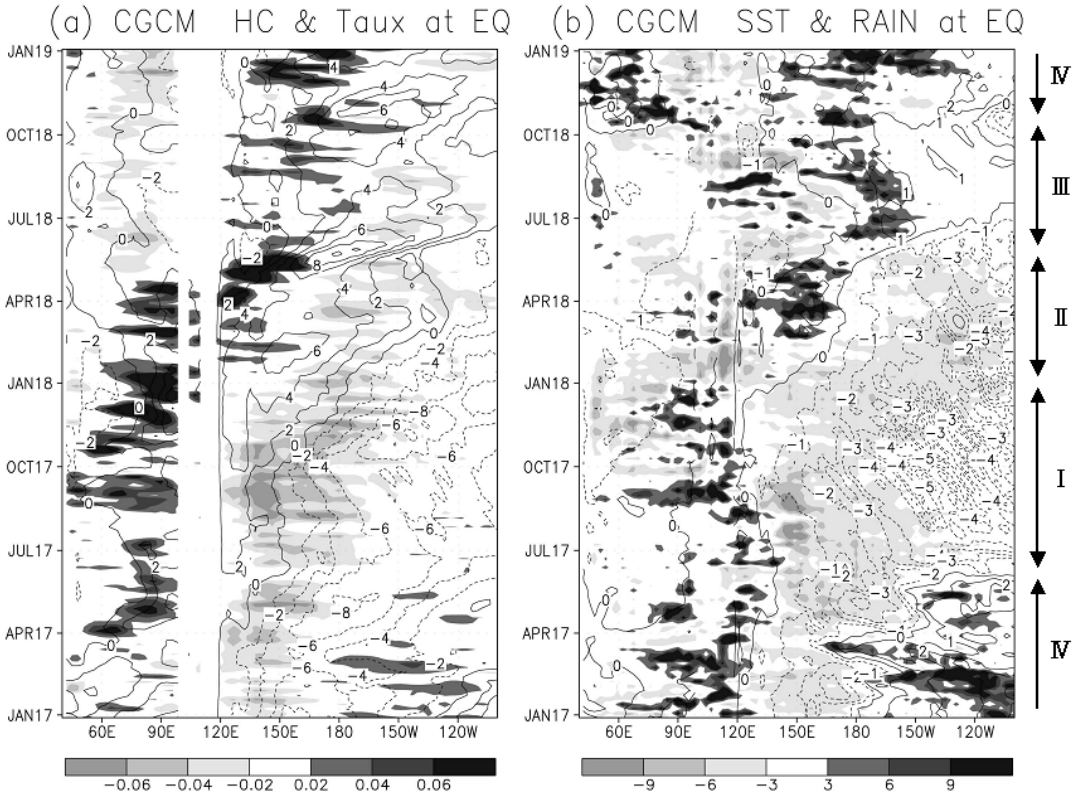

Fig. 13 (a) Time-longitude section of 5-day mean model heat content and zonal wind stress anomalies along the equator. Contour interval for heat content is 2×10^4 ºC cm. Heavy and light shadings denote regions of significant westerly and easterly wind stress anomalies, respectively. (b) Time-longitude section of 5-day mean model SST and rainfall anomalies. Contour interval for SST is 1ºC. Heavy and light shadings denote regions significant

positive and negative rainfall anomalies, respectively.